A PDA-Based Wireless Biosensor Using Industry Standard Components

Daniel R. Sommers, Desmond D. Stubbs, and William D. Hunt

Abstract—This paper presents the conception, design, implementation, and validation of an original, fully functional biosensor based on surface plasmon tesonance (SPR) technology. We present the motivation for building this sensor followed by the system specification, a brief overview of the theory of operation for SPR physics, and then give a detailed description of the hardware design, software design, and immunoassay design. We present a novel, graphical approach for tracking shifts in SPR center frequency with an autocorrelation feature that minimizes component variation. Additionally, we present the wireless communications aspects of our design, which adds to its appeal for remote system deployment and autonomous operation. Our success demonstrates the immediate availability of all the hardware, software, and biological components required to construct a fully functional biosensor with industrial application.

Index Terms—Immunoassay sensors, monoclonal antibody, surface plasmon tesonance (SPR), wireless biosensor.

I. INTRODUCTION

ONE VALIDATION technique for a new technology field, such as biosensors, is to build a practical device that has industrial appeal using only industry standard components. This technique validates both the existence of the requisite components and the maturity in the industry to define "practical." A short list of requirements from industry might be: easy to use, low cost, and rapidly deployed. Conversely, the overriding demand for research is high precision covering a broad range of applications.

For example, a biosensor that requires a lab full of graduate students to calibrate and operate (and for that matter, to interpret the results) would not meet the industry's criterion of "easy to use." Additionally, if a biosensor costs thousands of dollars with physical specifications measured in square meters and tens of kilograms, it is not likely to be considered "low cost" or "rapidly deployed."

In fact, broad industrial acceptance is predicated more on process than on theory of operation. A simple example is a home pregnancy test: if it is easy to administer and yields a result that is easily interpreted and reliable, the customer is satisfied.

Recently, the industry has been calling for "substance detectors" in applications ranging from protecting soldiers (and citizens) during biological warfare [1], [2] to preventing contamination or spoilage in food preparation and transport [3]. The common principle underlying these types of applications is that of detecting a shift in their environment from "normal" to "dangerous." Conveniently, the definitions of normal and dangerous are easily characterized and quantified so the challenge is to design a biosensor that can accurately measure and report changes in diverse environments.

II. BIOSENSOR SYSTEM DESIGN

A. System Specification

Based on industry demand, the sensor should have the capability to run continuously and monitor relevant changes in its environment. Further, it should be capable of tracking these changes in order to detect trends of both increase (alarm) and decrease (recovery) of the relevant changes. The sensor should be capable of running through multiple cycles of this type of activity. Finally, the sensor should be easily deployed in remote areas.

The high-level list of our requirements is as follows:

1) continuous monitoring;
2) high specificity for contaminant;
3) multiday, autonomous operation;
4) notification upon contaminant detection;
5) field deployable (portable, small, etc.).

The high specificity of antibodies makes them an ideal choice for a wide variety of sensor applications and they also satisfy the criterion of continuous monitoring and can function for weeks in a proper environment. The ready availability of small computer technology—from ultrathin laptops with wireless modems to programmable smart phones—can easily satisfy the requirements for autonomous operation and notification from a field location. The system must exploit some means of translating the biological signal of antibody activity to the digital world of the computer, and, finally, the notification mechanism should be industry standard (e.g., internet e-mail: any address containing "@").

B. Component Selection

The next step was to search the technologies currently available and select the best matches to our requirements.

1) Sensor Technology: Texas Instruments manufactures a surface plasmon resonance (SPR) [4] liquid sensor called the "*Spreeta*" [5]. The immediate appeal of the Spreeta biosensor is its low cost, low power requirements, and immediate availability in bulk quantities [6]. Further, SPR is capable of tracking changes, both increases and decreases, in antibody activity.

2) Computer Technology: Motorola, Inc., manufactures a programmable "smart phone" called the "*Accompli 009*." This

D. R. Sommers is with the Department of Biomedical Engineering, Georgia Institute of Technology, Atlanta, GA 30332 USA (e-mail: sommersd@welchallyn.com).

D. D. Stubbs is with the School of Chemistry and Biochemistry, Georgia Institute of Technology, Atlanta, GA 30332 USA (e-mail: desmond.stubbs@chemistry.gatech.edu).

W. D. Hunt is with the School of Electrical and Computer Engineering, Georgia Institute of Technology, Atlanta, GA 30332 USA (e-mail: bill.hunt@ee.gatech.edu).
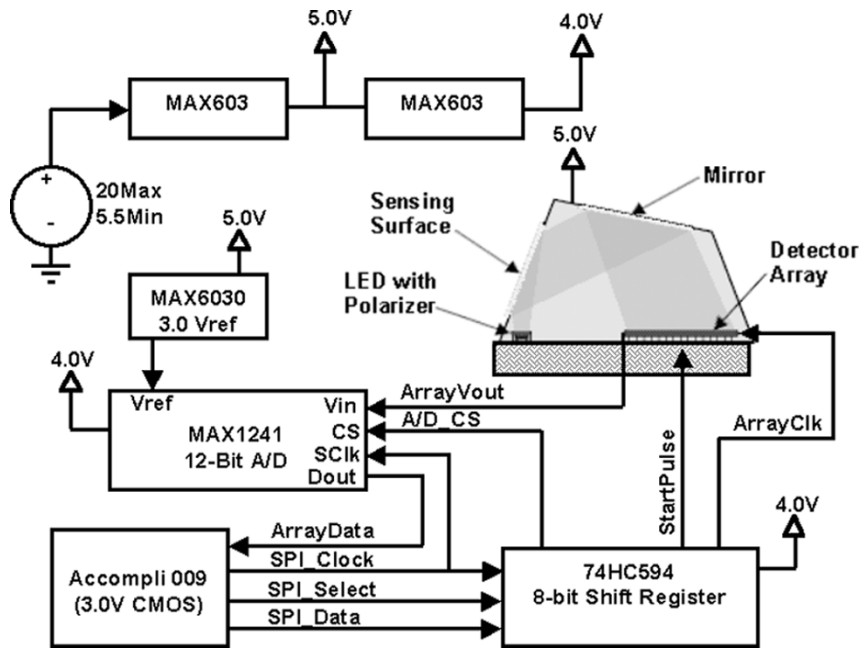
Fig. 1. Hardware block diagram.

device not only provides secure, wireless communication via e-mail, but it also sports a color screen, QUERTY keyboard, and a serial communications port for Spreeta attachment. This device is also optimized to run for days on a single, rechargeable battery and fits in the palm of the hand, features attractive to satisfy the "field deployable" requirement.

3) *Biological Technology*: the Sigma Chemical Company offers a vast library of monoclonal antibodies immediately available for purchase. Further, they are capable of manufacturing antibodies against specific analytes (contaminants) in the case that a suitable antibody cannot be found in their library. Using this source, our system can satisfy the requirements of continuous monitoring of biological analyte with high specificity and multiday capability.

C. System Operation Overview

After verifying the requisite components are all readily available from industry standard sources, we researched the basic operational capabilities of the system and defined the theoretical deployment of the system.

1) *SPR Theory of Operation*. The underlying principle behind SPR is that a thin layer of gold will act as a mirror and reflect light projected at it except under special "matching" conditions. At the resonant frequency, the light energy will not be reflected, but rather converted into mechanical energy, generating the plasmon waveform. Thus, by varying the frequency of the light striking the back of the gold film, a particular wavelength will match the precise permittivity on the front side. A direct plot of light frequency versus reflected light will show a marked loss of energy at the matching wavelength. The theory is explained further in the Appendix.

2) *Antibody Monolayer Theory of Operation*. The goal is to completely cover the gold SPR film with a consistent, continuous sheet of antibodies which have been grown to specifically bind only to the antigen of interest (Anthrax, cocaine,

etc.). When the analyte encounters the antibody, it will "stick" and, thereby, cause a perturbation in the permittivity, which will be measured with the SPR technology.

3) *Graphical User Interface*. The main output of an SPR system is a two-dimensional graph of light wavelength versus absorbed light. The system must be sensitive enough to measure shifts in the minimum value from one wavelength to another. Further, the user must be able to graphically set thresholds for the maximum shift, enter e-mail addresses for notification, and calibrate the average value output.

4) *Continuous Operation*. The system must monitor its environment continuously but conserve battery life. This requires two modes: a relatively slow "wake and sniff" mode which, upon detection of some interesting activity, will automatically switch to a "constant monitor" mode. Thus, the detection threshold must include a user-definable level that places the system on "alert status."

5) *Notification*. Upon detection of an SPR shift beyond the acceptable limits set during initialization, the system must generate a wireless notification to any number of preprogrammed recipients. If this alert is on a public network (e.g., cellular, paging, etc.), then the notification must be secured such that it can be neither lost nor spoofed.

III. HARDWARE DESIGN

The expansion port on the Motorola A009 is an industry standard serial peripheral interface (SPI) bus, which has three critical lines: data in, data out, and clock. The SPI bus integrates well with the Spreeta's synchronous clock design that drives the analog output sequentially from each cell in the array. Since the Spreeta provides only an analog output, the system requires an A/D converter. A 12-bit A/D converter can capture the dynamic range of the Spreeta (see Fig. 1).

Data is pumped sequentially from the 128 photocells of the Spreeta at each rising edge of its clock pin. The output then
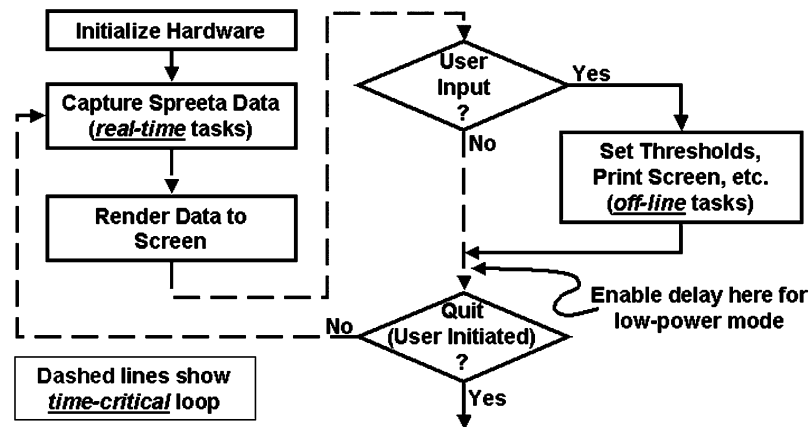
Fig. 2.   Main software loop.

attached to the 12-bit A/D must be read across the SPI bus into the Motorola Accompli 009. To overcome the lack of select lines on the SPI port, the design includes a serial-in-parallel-out shift register with staging capability. The SPI bus directly controls and clocks the shift register, which hierarchically controls and clocks the Spreeta and the A/D converter.

The final challenge was the power control design: the Spreeta is a 5-V device with a TTL-compatible interface and the SPI port is compatible with 3-V CMOS interface. By carefully selecting the voltage sources and interface logic on the shift register, we were able to avoid the propagation delay, real-estate, and power overhead of level shifters. Texas Instruments produces an HC version of the shift register which when supplied with 4-V can interface to both 3-V CMOS and 5-V TTL compatible devices.

All components are industry standard parts, most available from multiple suppliers. Because of the sensitivity of A/D converters to board noise, we chose linear regulators (MAX603 from Maxim, Inc.) and added high-quality tantalum decoupling capacitors on every component.

The final design consideration was to control the intensity of the light source within the Spreeta. We added a potentiometer to adjust the LED brightness and a software-controlled switch to turn it off which yields additional power savings when the Spreeta is not running its integration cycle.

IV. SOFTWARE DESIGN

The challenges in the software design were as follows:

1) maintaining real-time control of the Spreeta's light integration period in its photocell array;
2) processing the data from the Spreeta using strictly integer calculations;
3) defining a presentation mechanism with run-time analysis that yields instantaneous operational results and simple limit detection.

The software was designed with a hierarchy of tasks broken up into three categories: real-time, time-critical, and off-line (see Fig. 2). The real-time tasks are defined by the sensor hardware: the integration periods of the A/D converter and the Spreeta photocells. The time-critical tasks are defined by the "continuous operation" requirement and include screen updates and loop checks (e.g., check for user input). The off-line tasks

are all tasks that suspend the continuous operation of the sensor. These are typically user initiated (print screen, set threshold, etc.) with "alert user of threshold violation" being an example of nonuser initiated task.

A. Real-Time Tasks

The Motorola Accompli 009 has a real-time operating system that supports precise timing for the light integration period in Spreeta's photocell array and supports dedicating a hardware timer to the task. The timer period can be adjusted during normal operation, which sets the average value of all pixels, as well as moves the entire waveform horizontally within the graph (shorter $\Longrightarrow$ lower; longer $\Longrightarrow$ higher).

To maximize the precision of the integration period, the algorithm shuts off interrupts, waits for the user-programmed delay, then enters a loop of 128 cycles clocking each subsequent photocell value from the Spreeta to the A/D converter and reads in the A/D value (see Fig. 3). The delay clock resolution is 1 μs, which is sufficient to minimize the waveform jitter between cycles. The delay is initialized to 5 ms (5000 ticks) and can be incremented and decremented in 50-μs increments during normal operation. Note that the timer's minimum resolution is 30 ns, but clocking faster increases power consumption while only producing negligible improvements in jitter.

We invested significant effort to minimize the cycle through the real-time loop; unloading the 128 photocells from the Spreeta as quickly as possible after integration minimizes any effects of voltage leakage in the charge-coupled devices used to store the collected light. Our optimizations in this area resulted in a Spreeta clock rate of 45 KHz.

B. Time-Critical Tasks

The Motorola Accompli 009 provides programmable access only to the display processor; the DSP is dedicated to wireless communications and is therefore not accessible by user-loaded programs. This architecture imposes the constraint of "integer only" math because the display processor is sized for low cost and minimal power consumption, not intensive floating-point calculations. We designed a waveform-smoothing algorithm that requires only shifts and adds: the array of 128 light intensity values (I[128]) that correspond to 128 different wavelengths
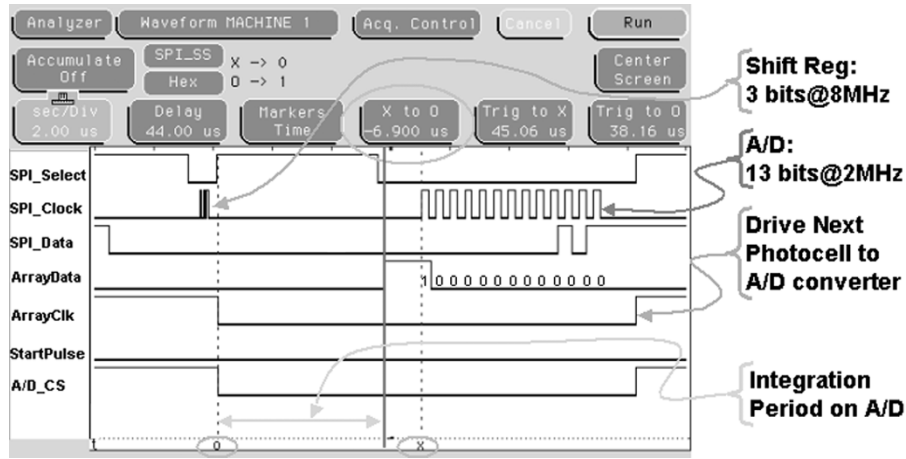
Fig. 3.   Logic analyzer capture: real-time control of Spreeta, A/D converter, and shift register on the SPI bus.

projected onto the gold film, were smoothed by the "C" pseudocode shown, as follows:

$$I[N] = (((I[N-1] + I[N-2] + I[N+1] + I[N+2]) \gg 2) + I[N]) \gg 1. \quad (1)$$

Thus, given a contiguous set of array data values (a, b, c, d, and e) with "c" being the value to smooth, this convolution algorithm produces the weighting shown in (2)

$$c_{\text{conv}} = \frac{\left(\left(\frac{a+b+d+e}{4}\right) + c\right)}{2}. \quad (2)$$

Numerically expressed, the weighting kernel is [0.125 0.125 0.5 0.125 0.125], which is a weighted average based on a geometric distance squared principle. The geometric distance square relationship would be a weighted progression of 1/2, 1/4, 1/16, etc., but for the sake of avoiding compute-intensive statistical smoothing, we chose the approximation presented above. The photodiode array in the Spreeta is mechanically discrete, and we commonly observed a 10–20 mV variance between adjacent array points that were not recording resonance (e.g., should have been a flat line). Note that the smoothing algorithm is applied to the "raw" data collected during the real-time phase, but the actual calculation is performed during the rendering phase which further minimizes the time spent in real-time processing.

After smoothing, the intensities are mapped directly onto the absolute graph which is 128 pixels wide yielding a 1-to-1 correspondence between intensities and the screen pixels along the X axis. The Y axis is a voltage scale and thus requires a conversion to the screen height [see Fig. 4(a)]. Floating point calculation was unavoidable for this case, but divides were converted to reciprocal multiples, which saved thousands of processor clocks per calculation and yielded a rate of approximately eight full cycles/second.

The final challenge was detecting curve shifts. The first solution was to allow the capture of an "initial" waveform and superimpose subsequent waveform cycles in red. This had the desired effect of showing shift continuously but with a minimum resolution of one pixel. Our novel solution for displaying SPR shift without requiring floating point calculation was to define a new waveform format we call "differential mode" [see Fig. 4(b)].
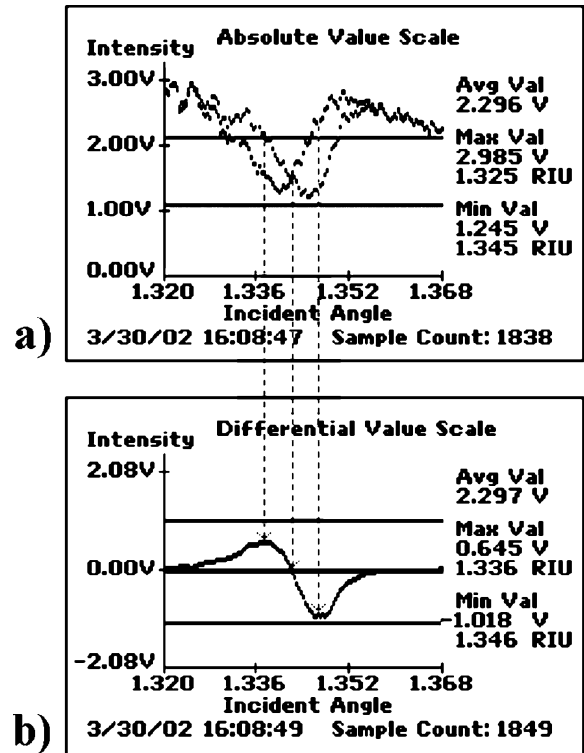

Fig. 4. Biosensor screens illustrating the relationship between the "differential" and "absolute" modes.

The differential waveform is generated by a simple 128 cycle loop subtracting "new" − "original" and plotting the difference to the screen, but it can be exploited as a powerful mechanism for watching an SPR shift occur during the continuous operation. It also yields the following:

1) a simple check for changes over time by marking the height of the differential curve over the "zero level;"
2) enforcement of a threshold with a simple check against the maximum and minimum threshold values;
3) autocorrelation of Spreeta output that normalizes waveform differences due to device variation.

A final advantage of the differential format is that we can control the values on the Y axis. By selecting values that were an
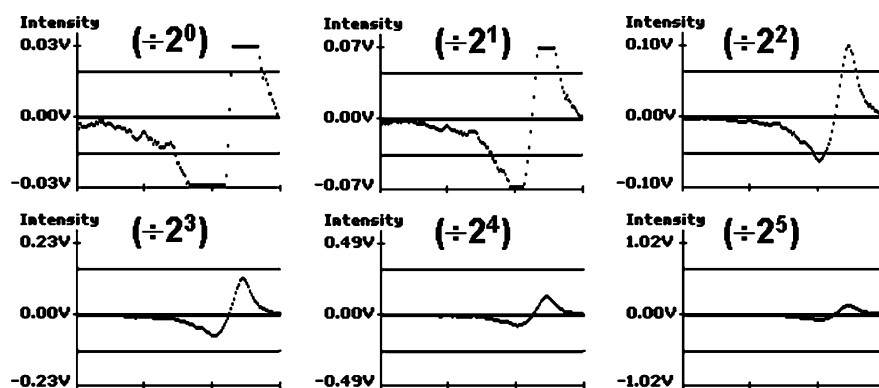
Fig. 5.   Differential screen progression showing the same waveform magnified (divided by) increasing powers of 2.

Fig. 6.   Screen shot of pop-up sending wireless e-mail notification upon detection of threshold violation.

even increment of a power of 2, we were able to map the voltages to screen values by a simple left-shift (e.g., voltages$/2^1 = $ voltages $\gg 1$; voltages$/2^2 = $ voltages $\gg 2 \ldots$ voltages$/2^9 = $ voltages $\gg 9$; $2^0 = $ no shift at all, see Fig. 5). Note that the voltages (intensities) may well be greater than the values at the Y axis in which case the algorithm simply "clips" the data and plots the maximum height for the scale. This simply represents saturation for the chosen display limits but is no loss of data: Simply dividing by a greater power of 2 will allow the data to be represented meaningfully on a graph with a broader range. By eliminating floating-point calculations in differential mode, the main loop runs at approximately 23 full cycles/second (a $3\times$ reduction in cycle time).

C. Off-Line Tasks

The off-line tasks suspend the normal operation of the sensor, perform the required task, and then resume normal operation. One of the longest tasks is sending the e-mail notifications upon detection of a threshold violation (Fig. 6). This routine will encrypt the user-entered message content and send it to the e-mail destination address list wirelessly over the public networks; secure [9] data with guaranteed delivery.

V. SYSTEM VERIFICATION

To verify that the design is operable, we employed an immunoassay previously used by our laboratory to verify acoustical sensors [10]. The procedure to build the immunoassay described in [10] and run an assay on the SPR biosensor is presented in brief here. This immunoassay consists of attaching a monolayer of mouse monoclonal antifluorescein isothiocyanate
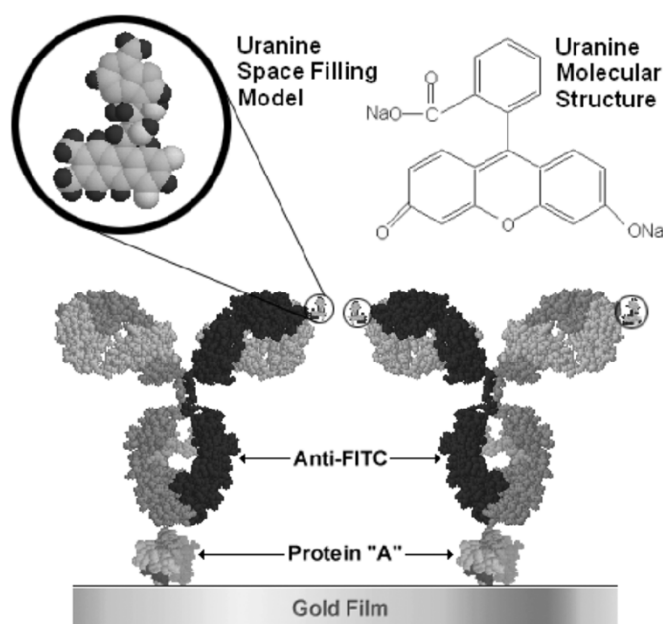

Fig. 7.   Monolayer stack-up on sensor surface.

(anti-FITC) antibodies from Sigma Chemical Company to the surface of the sensor. The anti-FITC molecule is attached to the biosensor surface via a well-known binding protein known as "protein a," purchased from Sigma-Aldrich Chemical Company. Before attachment the surface is prepared using 1 M NaOH and 1 M HCl, followed by washing with buffer. Protein a, a multivalent biomolecule, self assembles on gold surfaces and binds to the Fc (stem) of the antibody molecule; this ensures the correct orientation is maintained for analyte binding. The entire monolayer is illustrated in Fig. 7 including a representation of uranine molecules attached to the anti-FITC's antigen binding site.

Any analyte with a high affinity for anti-FITC will come out of solution and bind to the monolayer, thereby changing the effective permittivity within the SPR interrogation field. According to SPR theory, this change is detectable via a shift in the SPR resonant wavelength. Note that uranine and FITC have comparable binding affinities for anti-FITC and both are fluorescent, but since uranine is more soluble, it is a better choice for a liquid assay. A fluorescent immunoassay provides a convenient mechanism for cross-correlation of monolayer binding by first measuring the binding events using the biosensor, then
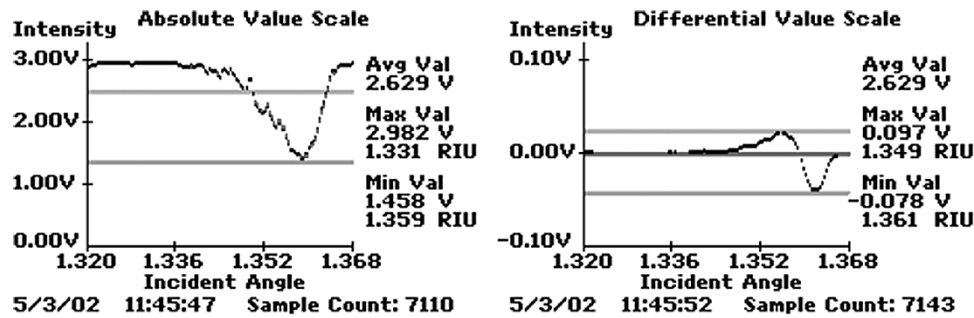
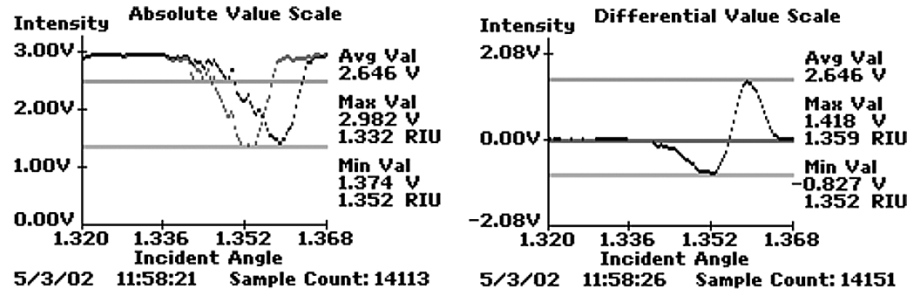Fig. 8.   Small SPR shift right during uranine binding experiments.

Fig. 9.   Large SPR shift left during uranine binding experiments.

exposing the sensor surface to UV light and measuring the intensity of the fluorescence.

Illustrated in Fig. 8 is one of the readings we captured during a uranine binding experiment. The data shown represents a slight shift to the right, which represents a slight decrease in permittivity. Note that, for this device, a decrease in permittivity invokes a shift to the right and an increase in permittivity a shift left. Based on this observation, we might be tempted to conclude that when uranine binds to anti-FITC, the binding induces a decrease in permittivity. However, we also captured the waveforms show in Fig. 9 during the same experiment.

Obviously, the results of both a large increase in permittivity and a small decrease in permittivity cannot both be the result of the same biological phenomenon. Therefore, we conclude that there are other factors contributing to the observed shift in permittivity. In its most general form, permittivity is described by a real component and a complex component. The real component represents a fixed arrangement of the atoms in a material and the complex component represents contribution by mobile ions. In calculating the dielectric constant for a thin-film capacitor, for example, the complex component can be ignored. However, the application of SPR to an antibody/analyte binding experiment should be strongly affected by free ions.

VI. DISCUSSION

The single light source in the Spreeta strikes the gold film at progressively sharper angles and only the component of the polarized light that is perpendicular to the surface interrogates the biolayer. Thus, we have come to think of it as 128 simultaneous SPR engines all operating at progressively increasing wavelengths. This must be clearly understood because a monolayer is never "text-book perfect" across the entire face of the sensor surface which would result in exactly one resonant frequency at all times.
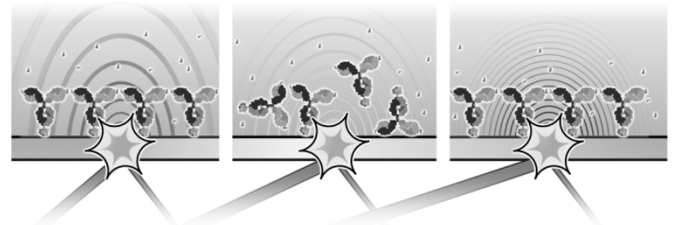

Fig. 10.   Multiple simultaneous induced plasmons.

As illustrated in Fig. 10, several locations along the face of the gold film can resonate simultaneously: resonance at the expected wavelength induced by the ideal conditions (far left), resonance at the wavelength interrogating a patch of nonspecific (random) binding, and resonance due to variations in interrogation depths caused by shorter wavelengths (far right). For the third example, consider a charge distribution gradient that is highest near the structure of the monolayer and gradually lessening as distance increases into the random particle distribution of the buffer. In such a gradient, the "blue shifted" interrogation will be stronger in the higher charge densities, but the "red shifted" interrogation will penetrate farther into the lower charge densities.

Our observations of the waveform output from the Spreeta correlate with this "multiple simultaneous resonance" theory in that we have clearly seen cases where the curve widened or narrowed, as opposed to strictly shifting right or left, indicative of a change in resonance in one region without a complimentary change at the opposing region. This observation was facilitated by the "raw" data graphs correlated with the differential graphs. Smoothing algorithms that resolve for the shift while ignoring the shape of the waveform are likely to hide this type of information. Thus, it is beneficial to study the "raw" data coming

from the Spreeta, which may be yielding quantitative information about the monolayer itself as opposed to just operational information about resonance shift. It may be yielding information on both shifting and "skipping" at the same time.

The final comment is on controlling permittivity. Since permittivity is a measure of the charge-holding and/or field-sustaining capability of a material, it is consistent with the basic theory of SPR that a change in free ion concentration would yield shift in resonance frequency. This is the reason the "negative" test of Alexa introduced to a monolayer of Anti-FITC failed to register "no activity" in an SPR sensor; a solution containing Alexa will have more free charge than the same solution containing a comparable concentration of uranine. Further, changes in pH, temperature, and even pressure change the concentration of free ions in the interrogation field.

As in most biosensor applications, the success and accuracy of the assay is based on sample preparation and environmental control. Often, it is not possible to control the temperature or the pH, but if those parameters do change during an assay, SPR theory clearly predicts these changes will register as shifts in the resonant frequencies. These shifts must be quantified and extracted as noise from experimental results.

VII. CONCLUSION

This research shows that it is possible to build a viable biosensor using only industry standard components commercially available. In fact, many of the hardware components used were requested as free samples on the websites of the companies which vend them [11], [12]. Texas Instruments also supplied the Spreeta devices free of charge in response to an e-mail request and Motorola also supplied the Motorola Accompli 009 and the software development environment without charge in support of this research project.

This biosensor can readily serve any application where the goal is to detect real-time drift away from a calibrated (e.g., "known good") starting point. In manufacturing process control, for example, this sensor can be immersed in vitro into a chemical processing flow and upon detection of a drift outside the calibrated limits (or, better yet, drifting toward violation of the calibration limits) the biosensor can wirelessly notify the system administrator and/or adjust the process' inputs.

This sensor can continuously monitor and, as a component in a feedback control environment, maintain the quality of the output. There are practical applications in food processing, drug manufacturing, oil refineries, and waste management. Note that this sensor is only suited to liquid applications and as implemented does not have direct application in any sort of "vapor phase" analysis.

APPENDIX
SPR THEORY OF OPERATION

SPR is a physical phenomenon for which the electrons in a thin gold film can be excited into a collective oscillation by bombarding it with photons (light) of a particular frequency. This phenomenon is analogous to resonant frequency in a mechanical system in that there must be a precise match between the light's frequency and momentum and the characteristics of the gold. Any mismatch between the wavelength of the
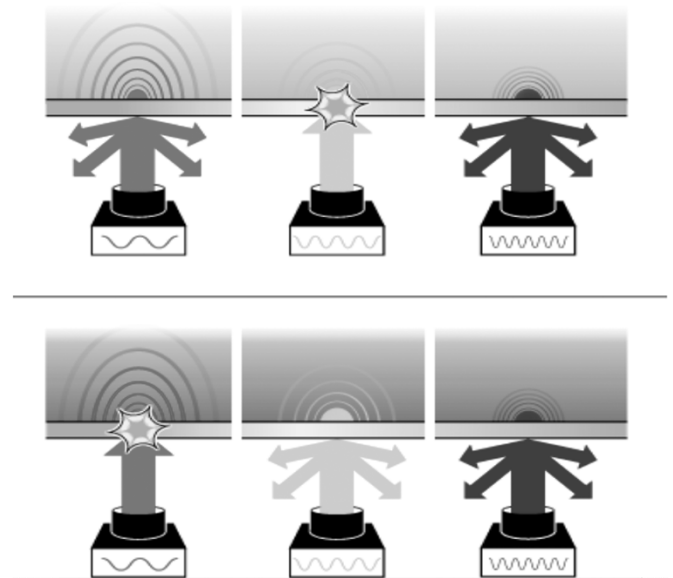

Fig. 11. Change in permittivity shifts SPR excitation.
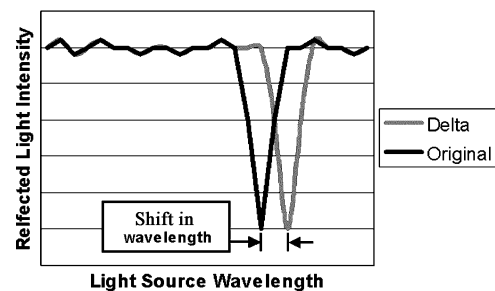
SPR Reflected Intensity vs. Wavelength

Fig. 12. Example of an "ideal" SPR shift waveform.

light: either too short (a.k.a. "blue-shifted") or too long (a.k.a. "red-shifted"), and the gold will fail to induce the plasma oscillation. The matching wavelength is also dependant on the permittivity of the material on the opposite side of the gold film (see Fig. 11).

Permittivity is a measure of a material's capability to store energy in an electric field and is defined in terms of the material's dielectric constant. In a thin film, the light actually induces an interrogation field on the opposite side of the gold. This field interrogates the relative permittivity for a distance on the order of one wavelength of the light striking the surface. A biological system is not likely to be disturbed by an electromagnetic field. A biological system can, however, invoke a change in permittivity. This change of permittivity within the interrogation field of the SPR system can cause a measurable shift in the wavelength required to excite the plasma state (see Fig. 12).

ACKNOWLEDGMENT

The authors would like to thank the folks at Motorola, Texas Instruments, and Nomadics who answered their many questions and kept them moving forward on this project. A photograph of the fully functional prototype, including some of the development tools used to build it, is shown in Fig. 13. Note that although the Motorola Accompli has the appearance of a lap-top,

Fig. 13.   Photograph of fully operational biosensor prototype.

it is actually quite small and fits easily into the palm of the hand. They would also like to thank A. Runton who transformed their "back-of-the-envelope" drawings into the illustrations that, in their opinion, are worth far more that a mere thousand.

REFERENCES

[1] National Research Council: Division on Engineering and Physical Sciences, *Making the Nation Safer: The Role of Science and Technology in Countering Terrorism*.   Washington, DC: National Academy, 2002, pp. 113–117.
[2] S. P. Layne, T. J. Beugelsdijk, and C. K. N. Patel, *Firepower in the Lab: Automation in the Fight Against Infectious Diseases and Bioterrorism*.   Washington, DC: Joseph Henry, 2001, pp. 143–164.
[3] K. G. Ong, K. Zeng, and C. A. Grimes, "A wireless, passive carbon nanotube-based gas sensor," *IEEE Sensors J.*, vol. 2, pp. 82–88, Apr. 2002.
[4] E. Kress-Rogers, *Biosensors and Electronic Noses*.   Boca Raton, FL: CRC, 1997, ch. 7.
[5] Texas Instrument's Spreeta SPR Biosensor Technology Overview, Texas Instruments, Inc., Dallas, TX (2002). *http://www.ti.com/spreeta* [Online]
[6] Nomadics' Surface Plasmon Resonance Evaluation Kit, Nomadics Inc., Stillwater, OK (2002). *http://www.aigproducts.com/surface_plasmon_resonance/spr.htm* [Online]
[7] Motorola's Accompli 009 Personal Communicator Product Overview, Motorola, Inc., Schaumburg, IL (2002). *http://www.motorola.com/accompli009* [Online]
[8] Sigma-Aldrich Chemical Company, St. Louis, MO (2002). *http://www.sigmaaldrich.com/* [Online]
[9] NIST Certification for Motorola Accompli 009 for FIPS 140-1. *http://cs-www.ncsl.nist.gov/cryptval/140-1/1401val.htm* [Online]
[10] D. D. Stubbs, W. D. Hunt, S. H. Lee, and D. F. Doyle, "Gas phase activity of anti-FITC antibodies immobilized on a surface acoustic wave resonator," *Biosens. Bioelectron.*, to be published.
[11] Maxim Samples and Literature Request Page, Maxim Integrated Products, Sunnyvale, CA (2002). *http://www.maxim-ic.com/samples* [Online]
[12] Texas Instruments Sample Request Page, Texas Instruments, Inc., Dallas, TX (2002). *http://www.ti.com/sc/docs/sampreq.htm* [Online]

Daniel R. Sommers received the B.S. degree in computer and electrical engineering from Purdue University, West Lafayette, IN, in 1984 and the M.S. degree in computer engineering from Florida Atlantic University, Boca Raton, in 1996. He is currently pursuing the M.S. degree in bioengineering from the Georgia Institute of Technology, Atlanta.

He has 20 years of industry experience in telecommunications and computer design in both the hardware and software disciplines. He is currently with Welch Allyn, Inc., where he is the Embedded Systems Architect for the medical division. His interests are molecular diagnostics, sensor interfaces, and embedded control systems for medical applications.

Desmond D. Stubbs was born in Nassau, Bahamas, 1972. He received the B.S. degree in chemistry from Morris Brown College, Atlanta, GA, in 1997 and the M.S. degree in biochemistry from the Georgia Institute of Technology, Atlanta. He is currently pursuing the Ph.D. degree at the School of Chemistry and Biochemistry, Georgia Institute of Technology. His doctoral thesis involves engineering proteins for biosensor applications.

From 1999 to 2001, he was a demonstrations Teacher in the School of Chemistry, Georgia Institute of Technology.

William D. Hunt received the B.S. degree from the University of Alabama, Tuscaloosa, in 1976, the M.S. degree from the Massachusetts Institute of Technology (MIT), Cambridge, in 1980, and the Ph.D. degree from the University of Illinois, Urbana-Champaign, in 1987, all in electrical engineering.

Prior to his entrance into MIT's graduate program, he was an Engineer with Harris Corporation. Following completion of the M.S. degree, he joined the engineering staff at Bolt Beranek and Newman Corporation. He joined the electrical engineering faculty at the Georgia Institute of Technology, Atlanta, following completion of the Ph.D. degree.

Dr. Hunt received the NSF Presidential Young Investigator Award in 1989, the DuPont Young Faculty Award in 1988, and the University of Alabama Distinguished Engineering Fellowship in 1994. He was a Rhodes Scholar Finalist in 1975. His area of expertise is in the area of microelectronic acoustic devices for wireless applications, as well as chemical and biological sensors based on this technology. He has published over 70 papers in refereed journals and conference proceedings. He holds four U.S. patents and five provisional patents.